Hydrogen Storage in Decorated Multiwalled Carbon Nanotubes by Ca, Co, Fe, Ni, and Pd Nanoparticles under Ambient Conditions

ARTICLE *in* THE JOURNAL OF PHYSICAL CHEMISTRY C · MARCH 2011

Impact Factor: 4.77 · DOI: 10.1021/jp108797p

6 AUTHORS, INCLUDING:

Ali Reyhani
Imam Khomeini International University
35 PUBLICATIONS **362** CITATIONS
SEE PROFILE

S. Zahra Mortazavi
Imam Khomeini International University
52 PUBLICATIONS **358** CITATIONS
SEE PROFILE

Soghra Mirershadi
University of Mohaghegh Ardabili
15 PUBLICATIONS **194** CITATIONS
SEE PROFILE

Parviz Parvin
Amirkabir University of Technology
164 PUBLICATIONS **618** CITATIONS
SEE PROFILE

THE JOURNAL OF PHYSICAL CHEMISTRY C

ARTICLE

pubs.acs.org/JPCC

Hydrogen Storage in Decorated Multiwalled Carbon Nanotubes by Ca, Co, Fe, Ni, and Pd Nanoparticles under Ambient Conditions

A. Reyhani,[†] S. Z. Mortazavi,[‡] S. Mirershadi,[†] A. Z. Moshfegh,[*,§,⊥] P. Parvin,[‡] and A. Nozad Golikand[†]

[†]Material Research School, P.O. Box 14395-836, Tehran, Iran

[‡]Department of Physics, Amirkabir University of Technology, P.O. Box 15875-4413,Tehran, Iran

[§]Department of Physics, Sharif University of Technology, P.O. Box 11155-9161, Tehran, Iran

[⊥]Institute for Nanoscience and Nanotechnology, Sharif University of Technology, P.O. Box 14588-8969, Tehran, Iran

ABSTRACT: We report a study on hydrogen storage in Ca, Co, Fe, Ni, and Pd decorated multiwalled carbon nanotubes (MWCNTs) by using two techniques: volumetric and electrochemical. The results showed that hydrogen molecules are adsorbed on the defect sites and transported to the spaces between adjacent carbon via diffusion through both defect sites and opened tips into the layers. Hydrogen storage capacity can be improved in the decorated MWCNT by Co, Fe, Ni, and Ca metals in two approaches: (i) H_2 adsorption via Kubas interaction and (ii) dissociation of H_2 molecules on the metal particles. The results reveal that Pd are more effective catalyst for hydrogen storage process. It was found that dissociation of H_2 occurs on the Pd particle, and hydrogen atoms are entered into the spaces between adjacent carbon layers. They create loosely bonds of CH_x species and Pd−C−H_x complex which can be decomposed easily at lower temperatures as compared to C−H chemical bonds.

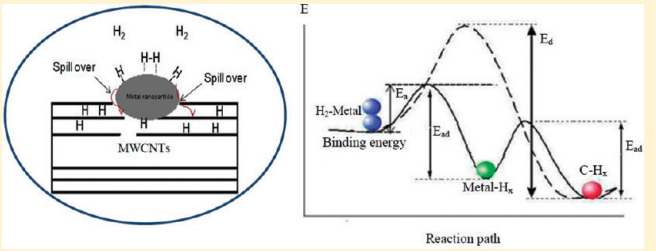

1. INTRODUCTION

Finding alternative energy resources to substitute for mineral energy sources has been a very important issue due to serious problems including air pollution and release of greenhouse gases as well as shortage of energy with increasing the world population. Thus, to obtain a fully renewable and environmentally safe energy source, many scientists and researchers have been extensively investigated to ease the problem in recent years.[1−3] Hydrogen is a promising clean energy carrier and has been attracting much interest from the scientific and technological viewpoints.[4] In this context, high-capacity storage of hydrogen with a safe, effective, and cheap system at temperature ranging from near ambient to about 100 °C and at pressures below ∼100 bar is essential in practical applications.[1−5] These conditions favor storage based on the interaction of hydrogen with solid materials, rather than the compressed or liquid hydrogen, storage which requires high pressures (700 bar) or low temperatures (20 K), respectively.[4,5]

Carbon-based materials, due to their low cost and weight, have long been considered as suitable adsorption substrates for the reversible storage of hydrogen; however, hydrogen storage in these materials is still at a research level and is not yet mature enough for industrial application.[6,7] Since the report of Dillon et al.[8] on a possible 5−10% hydrogen storage capacity for single-walled carbon nanotubes (SWCNTs), carbon nanotubes (CNTs) have attracted considerable interest due to the usage of CNTs as a safe hydrogen storage medium.[9,10] Significantly higher storage can be achieved in CNT by surface functionalization in two approaches: (i) via creation of nanometer-sized pores that dramatically raise both the surface area for adsorption and create deeper potential wells[7,11] and (ii) by doping with elements capable of strengthening the hydrogen−substrate interaction.[7,12]

Recently, many studies have revealed that hydrogen storage capacity is enhanced by added metals to carbon structures such as Ag, B, Ca, Fe, K, Li, Ni, Pd, Pt, Ru, Ti, TiO_2, and V.[6,13−33] Gao et al.[19] also indicate that fresh CNTs could only store 0.1 wt % of hydrogen at 573 K and ambient pressure; however, oxidation treatment to produce defects and subsequent loading with a Pd−Ni catalyst significantly increases the hydrogen storage capacity up to 6.6 wt % at 610 K and ambient pressure. Singh et al.[34] reported the high hydrogen storage capacity of metallacarboranes, which the light transition metal (TM) atoms can bind up to 5 H_2 molecules via Kubas interaction. Liu et al.[35] studied a high uptake H_2 capacity of 13.45 wt % for the Li-dispersed carbon nanotubes system using density functional theory (DFT) calculations. They concluded that binding strength and uptake capacity of the carbon nanotubes can be enhanced by introducing more dopants due to electron transfer from Li atoms to carbon atoms. This finding was also reported for Ca[34,36] and transition metals[37] by the other researchers.

In the present work, we explore the influence of added different metal including Ca, Co, Fe, Ni, and Pd to multiwalled

Received: September 15, 2010
Revised: February 14, 2011
Published: March 18, 2011

carbon nanotubes (MWCNTs) for improving hydrogen adsorption property at ambient pressure and temperature. Pd is investigated to be a suitable catalyst to absorb, dissociate, and store hydrogen in the spaces between adjacent carbon layers. Moreover, the hydrogen adsorption mechanism and hydrogen adsorption sites of the MWCNTs and metal-doped MWCNTs are studied. Scanning electron microscopy (SEM), transmission electron microscopy (TEM), thermal gravimetric analysis (TGA), differential scanning calorimetry (DSC), energy dispersive analysis X-ray (EDAX), X-ray photoelectron spectroscopy (XPS), and Raman spectroscopy were used to evaluate the structure, degree of graphitization, quality, and adsorption characteristics of both the MWCNTs and metal-doped MWCNTs.

2. EXPERIMENTAL SECTION

2.1. Catalyst Preparation and MWCNT Growth. Fe/Ni/MgO catalyst with the proportion of 1/1/8 was used for the growth of MWCNTs using the thermal chemical vapor deposition (TCVD) method. All materials were obtained from Merck Co. The experimental details of catalyst preparation and MWCNT growth have been reported elsewhere.[38]

2.2. Purification and Functionalization of MWCNTs. Purification of the MWCNTs was performed first by HF and then by H_2SO_4 and followed by HNO_3. First, the raw MWCNTs were placed in the boat, calcined in the furnace at 450 °C for 60 min in O_2 ambient, and then cooled down to room temperature. Some 100 mg of the oxidized MWCNTs was immersed in 3 M solutions of HF for 24 h at room temperature. Subsequently, the MWCNTs were immersed in 3 M solutions of sulfuric acid and then nitric acid at their boiling temperature each for 6 h. Finally, the MWCNTs were washed out several times with deionized water until the pH value of the solution became neutral. The samples were then dried at 150 °C for 24 h in ambient. For functionalization of the MWCNTs, 100 mg of the purified MWCNTs and 1 mol of Ca, Co, Fe, Ni, and Pd nitrates were immersed in distilled water, and the mixture was stirred for 1 h. Then, the ionic-adsorbed MWCNTs were separated from the metal salt solutions using a filtration. Finally, the obtained metal-doped MWCNTs were heated at 200 °C for 24 h.

2.3. Sample Characterization. Characterization of the synthesized MWCNTs was carried out by the following techniques: SEM (XL30, Philips) and TEM (XL, Philips) were used for determining the morphology and diameter of MWCNTs. TGA and DSC were employed to investigate MWCNT yield and the degree of graphitization using simultaneous thermal analysis (STA). The heat treatment was considered in a temperature range from 30 to 850 °C with the heating rate of 10 °C/min in air ambient. Raman spectroscopy (HR-800, Jobin-Yvon) was utilized to determine the quality of purified MWCNTs. The Raman spectra were recorded in a range from 200 to 2000 cm^{-1} with 0.1 cm^{-1} accuracy. Elemental composition of the MWCNTs was determined by EDAX (XL30, Philips). The surface functional groups of the MWCNTs were identified by XPS equipped with Al Kα X-ray source at energy of 1486.6 eV using a concentric hemispherical energy analyzer (Specs EA 10 plus). All of the peaks were deconvoluted using SDP software (Version 4.1) with 80% Gaussian−20% Lorentzian peak fitting. The XPS measurements were performed in the analysis chamber operating in a vacuum better than 10^{-7} Pa.

2.4. Hydrogen Storage. Volumetric and electrochemical techniques were used to determine the hydrogen storage capacity of the synthesized MWCNTs. In the volumetric study, 100 mg of the MWCNTs was placed in a quartz tube. The experimental details of hydrogen storage by the volumetric technique have been reported in ref 38. For studying the hydrogen storage of the MWCNTs by the electrochemical technique, 2 mg of the MWCNTs was used as the working electrode. Details on fabrication of the electrodes can be found in our previous report.[39] For testing the hydrogen storage of the MWCNTs, the working electrode was charged for 20 min at the constant current of 3 mA and discharged under the similar conditions.

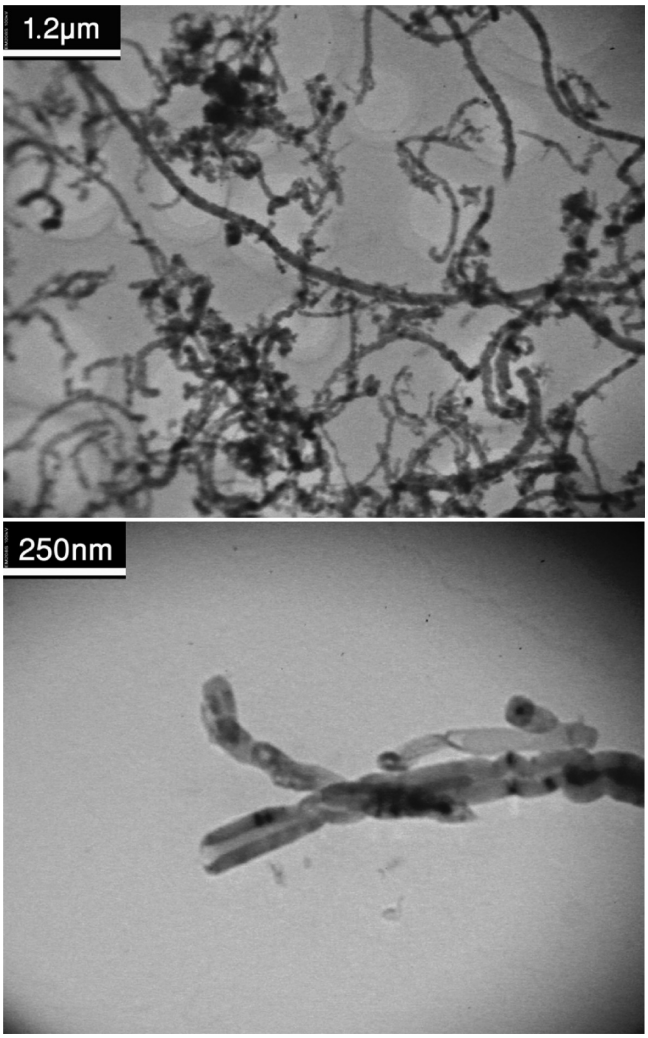

Figure 1. TEM images of the pure MWCNTs.

3. RESULTS AND DISCUSSION

The TEM (XL, Philips) micrographs of the pure MWCNTs and Pd-doped MWCNTs are shown in Figures 1 and 2. As the figures depict, the average diameter of the purified MWCNTs is about 60 nm. It indicates that some of MWCNTs are open tip. It was noted that the long-range ordered structure in the tube wall was not well developed. The TEM images of Pd-MWCNTs (Figure 2) reveal the Pd particles formed on the defect sites. Raman spectroscopy (HR-800, Jobin-Yvon) was also used to determine the quality of the MWCNTs. The Raman spectrum was recorded in a range from 200 to 2000 cm^{-1} with 0.1 cm^{-1}

accuracy. In fact, the I_G/I_D intensity ratio of the peaks is used as a rough measure of the sample quality.[40] The ratio of the purified MWCNTs was about 2.1. Therefore, about 30% of the purified MWCNT structures used in this study involve the defect structures such as dangling bands and carboxyl groups. This result of Raman spectroscopy is in good agreement with our TEM observations. Many researchers reported that defect sites in CNTs could adsorb hydrogen molecules accompanying a considerable increase in both adsorption binding energy and desorption temperature, which will definitely affect the molecular hydrogen storage capacity in comparison to ideal hexagonal structures of CNTs.[39,41,42]

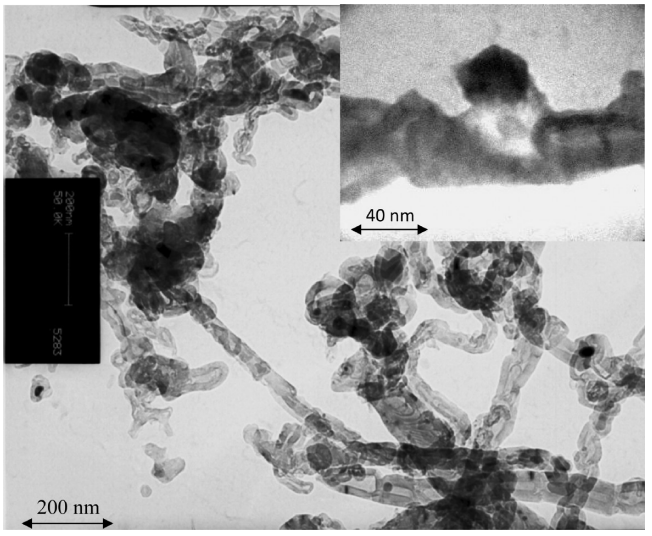

Figure 2. TEM images of the Pd-doped MWCNTs.

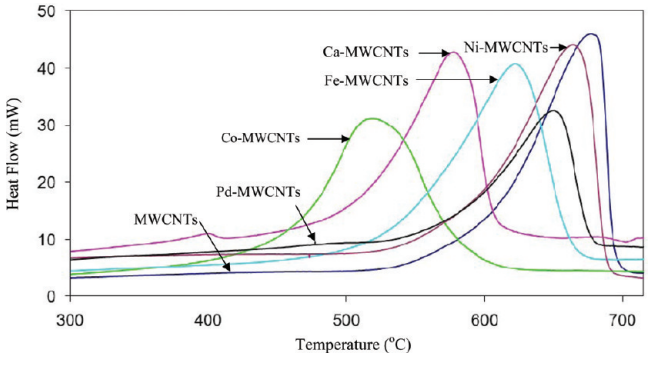

Figure 3. DSC analyses of the purified MWCNTs and Ca, Co, Fe, Ni, and Pd-doped MWCNTs.

TGA and DSC curves derived from simultaneous thermal analysis (STA) were used to determine the yield and the graphitization degree of the MWCNTs. The heat treatment was considered in a temperature range from 30 to 850 °C with the heating rate of 10 °C/min in air ambient. The yield of MWCNTs was obtained using their weight loss percentage in a temperature range from 500 to 800 °C.[22] TGA and DSC results of the purified and doped MWCNTs by Ca, Co, Fe, Ni, and Pd are shown in Figure 3 and Table 1. The high yield of the purified MWCNTs (93.5%) shows that the acid treatment decreased catalyst particles and MgO support in the sample.[15] The reduction of weight loss (%) for metal-doped MWCNTs explained that they are functionalized by all the investigated metals. DSC results of Ca, Co, Fe, Ni, and Pd-doped MWCNTs showed that the oxidation process started at lower temperature as comprared with the purified ones. This is because the oxidation of MWCNTs is catalyzed by metal doping as compared with the purified ones. Yoo et al.[16] and also in our pervious work[15] have reported a similar phenomenon by using La and Fe catalysts, respectively. EDAX (XL30, Philips) analysis was employed to determine elemental composition of the purified and doped MWCNTs. Results of the purified MWCNTs as well as Ca-doped and Pd-doped ones are shown in Figure 4. The

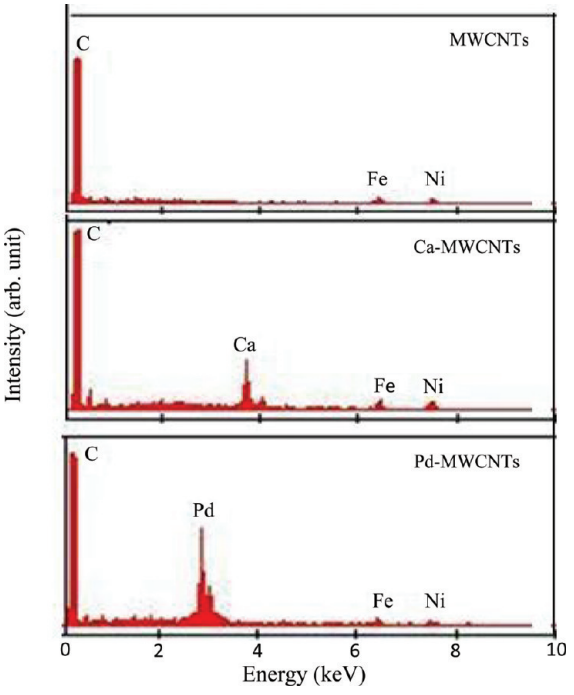

Figure 4. EDAX analyses of the purified MWCNTs as well as Ca- and Pd-doped MWCNTs.

Table 1. Results of TGA and DSC of the Purified and Metal-Doped MWCNTs

MWCNTs samples	onset temp (°C)	inflection temp (°C)	offset temp (°C)	weight loss (%) from 500 to 800 °C
CNTs	513.4	680.5	707.5	93.5
Ca-CNTs	435.4	579.9	625.5	85.1
Co-CNTs	382.3	524.4	619.4	88.2
Fe-CNTs	475.9	624.6	677.9	88.5
Ni-CNTs	502.3	666.1	697.6	86.2
Pd-CNTs	518.1	652.9	687.1	84.2

dx.doi.org/10.1021/jp108797p |J. Phys. Chem. C 2011, 115, 6994–7001

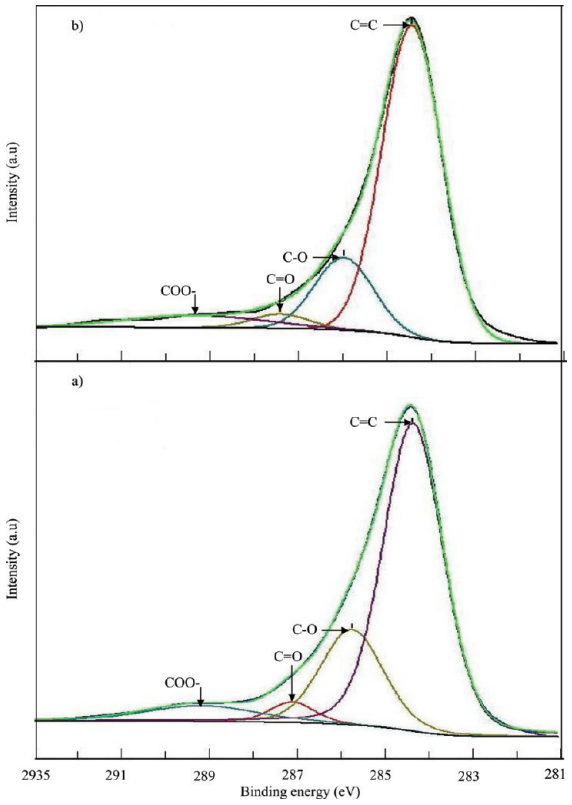

Figure 5. XPS spectra of the C(1s) core level for different situations: (a) purified MWCNTs and (b) Pd-doped MWCNTs.

Table 2. Contribution of Surface Functional Groups for the Purified and Pd-Doped MWCNTs Using XPS Analysis

samples	C═C (%)	C−O (%)	COO (%)	C═O (%)
MWCNTs	67.6	22	3.5	6.9
Pd-MWCNTs	73.3	16.8	3.2	6.7

obtained results were also confirmed by our TGA and DSC measurements (see Table 1).

In order to prevent the possibility of metal clustering, particular forms of defects in graphene (oxygen containing structurals) and BC_3 structures were suggested for effective metal dispersion with no clustering formation.[6,33,43] Therefore, XPS analysis was directly employed for investigating the surface functional groups of the MWCNTs and Pd-MWCNTs. The XPS results of these two systems are shown in Figure 5 and summarized in Table 2. The XPS measurements were performed in the analysis chamber operating in a vacuum better than 10^{-7} Pa with Al Kα X-ray source at energy of 1486.6 eV using a concentric hemispherical energy analyzer (Specs EA 10 plus). Figure 5a,b shows large peak at 284.5 eV (sp^2 C═C) and three smaller shoulders at around 286 eV (C−O), 287 eV (C═O), and 289 eV (COO).[44−46] The deconvoluted XPS spectra of the C(1s) demonstrate that the purified MWCNTs have a higher number of surface functional groups such as carboxyl, alcohol, and carbons neighboring to oxygen functional groups than the Pd-MWCNTs sample. Thus, the surface functional groups of the Pd-MWCNTs are reduced by specific interactions between the Pd particles and the oxygen functional groups in compared with the purified MWCNTs. That is why the

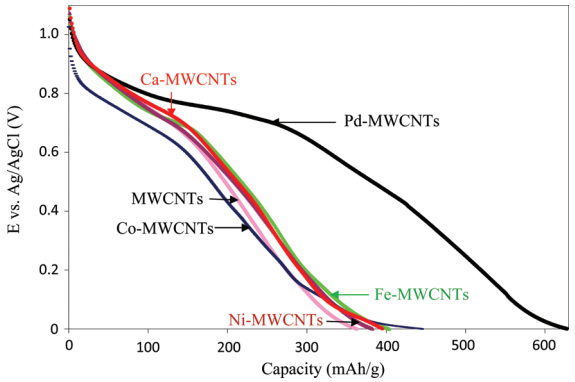

Figure 6. Discharge curves of the electrodes assembled with the purified MWCNTs and Ca, Co, Fe, Ni, and Pd-doped MWCNTs at the charge constant current of 3 mA for 20 min and discharge constant current of −3 mA.

Pd particles are tailoring on the defect sites in the walls of MWCNTs. This finding was also confirmed with TEM analysis. A similar result was also reported by Itoh et al. for the Pd-ox single-wall carbon nanohorns (SWCNHs).[44] Wang et al.[33] also found that Ti atoms bind strongly to the oxygen sites while clustering does not happen.

Hydrogen storage property of the purified MWCNTs as well as Ca, Co, Fe, Ni, and Pd-doped MWCNTs were measured by electrochemical technique. Figure 6 illustrates the discharging curves of the purified MWCNTs and the metal-doped MWCNTs. The reversible hydrogen storage capacity of the MWCNTs, Ca-MWCNTs, Co-MWCNTs, Fe-MWCNTs, Ni-MWCNTs, and Pd-MWCNTs was determined about 1.45, 1.58, 1.78, 1.62, 1.54, and 2.52 wt % corresponding to 363, 396, 445, 405, 385, and 630 mAh g^{-1}, respectively. For rechargeable samples, an important requirement is the capacity retain ability after certain charge−discharge cycles. The obtained results indicated that after six cycles of charge−discharge the capacity loss is negligible for all samples. As shown in Figure 6, the Pd-doped MWCNTs demonstrate the highest hydrogen storage capacity among the other studied MWCNT samples. This result reveals that Pd is an effective catalyst for hydrogen storage in the MWCNTs. A similar result has been also reported by other researchers.[17,18,24−26] The figure also shows that the hydrogen desorption process is composed of two steps with voltages at about −0.75 and −0.15 V.

Hydrogen storage property and capacity of the purified MWCNTs and also doped MWCNTs were also measured by the volumetric technique (Figure 7). The hydrogen storage capacity of the MWCNTs, Ca-MWCNTs, Co-MWCNTs, Fe-MWCNTs, Ni-MWCNTs, and Pd-MWCNTs under ambient conditions were determined as 0.3, 1.05, 1.5, 0.75, 0.4, and 7 wt %, respectively. This result was also confirmed by our electrochemical hydrogen storage of the MWCNTs as illustrated in Figure 6. To study different results obtained by volumetric and electrochemical techniques, it is well established that H_2 adsorption conditions are different in these two techniques. In addition, in the electrochemical H_2 storage technique, H_2O medium is utilized whereas in the volumetric measuring technique, H_2 atmospheric pressure is applied. Therefore, it is expected to obtain different H_2 storage capacities by these two techniques. However, it is important to note in both techniques the Pd-MWCNTs system exhibits the highest H_2 storage capacities as

dx.doi.org/10.1021/jp108797p |J. Phys. Chem. C 2011, 115, 6994–7001

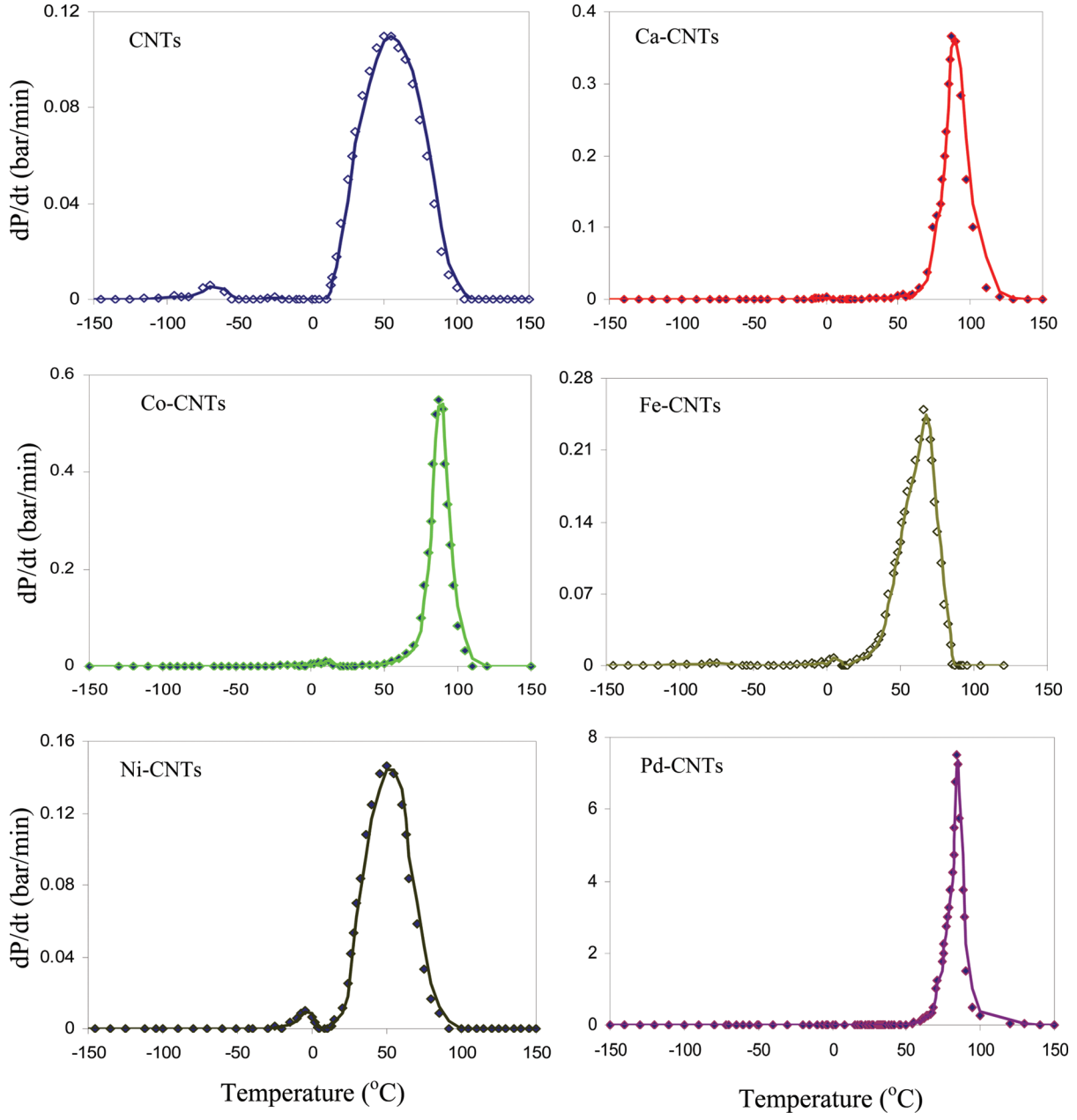

Figure 7. Volumetric data for the hydrogen storage capacity in purified MWCNTs and Ca, Co, Fe, Ni, and Pd-doped MWCNTs.

compared to other investigated systems. Difference in H_2 storage capacity measured by electrochemical and volumetric techniques was also reported by other researcher.[47,48] A summary of hydrogen storage results for the purified and doped MWCNTs is given in Table 3. The Arrhenius equation, $r_d \sim r_0 \exp(-E_d/kT)$, was also applied for calculating activation energy of hydrogen desorption for the second desorption peak in the different samples (Table 3). In the Arrhenius equation, r_d, r_0, E_d, k, and T are the desorption rate, pre-exponential factor, activation energy of hydrogen desorption, Boltzmann constant, and absolute temperature, respectively.[49] For further verification of reversibility of our samples (adsorption−desorption cycles), we have examined hydrogen storage capacity as a function of different number of cycles. Figure 8 depicts the cycling characteristics of the MWCNTs, Co-MWCNTs, and Pd-MWCNTs using the volumetric technique. It is clear that after six cycles of adsorption−desorption the capacity loss is negligible for the both MWCNTs and Co-MWCNTs, whereas hydrogen storage capacity loss for the Pd-MWCNTs system is found about to be 55%. The reduction of H_2 storage capacity was also observed for the Pd-MWCNTs system by other researchers.[16]

The results also indicated that there are two temperature regions for hydrogen adsorption on the purified MWCNTs: one at about −70 °C and the other at about +10 °C. Many researchers reported that H_2 desorption activation energy of C−H bindings in CNTs is about 2 eV per C−H bond, about half of the C−H covalent bond energy of CH_4 molecule.[50,51] Nikitin et al.[50] indicate that more than two-thirds of the C−H bonds in the hydrogenated SWCNT film dissociate at a temperature below 300 °C. They concluded that chemisorbed hydrogen as

Table 3. Hydrogen Storage of the Purified and Different Metal-Doped MWCNTs by the Volumetric Technique

samples	onset desorption emp peak (°C)	fwhm (°C)	desorption activation energy (kJ/mol)	hydrogen storage capacity (wt %)
CNT	10	60	39	0.3
Ca-CNTs	58	17	69	1.05
Co-NTs	56	12	65	1.51
Fe-CNTs	15	28	48	0.75
Ni-CNTs	14	40	47	0.4
Pd-CNTs	62	11	71	7

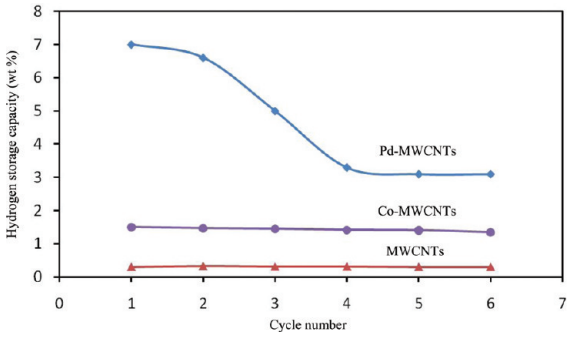

Figure 8. Cycle life performance of the MWCNT, Co-MWCNTs, and Pd-MWCNTs.

C−H binding desorbs from the SWCNT surface at temperatures in the range between 200 and 300 °C. Gao et al.[19] investigated hydrogen storage by chemisorptions on MWCNTs. They have reported that the chemisorbed hydrogen on the MWCNTs (C−H) desorbs in temperature more than 550 K. Wu et al.[41] studied that there are two peaks regarding desorption of adsorbed hydrogen in DWCNTs. One starts at about 300 K, while the other is at about 750 K. They are likely attributed to the combination of physical absorption (starts from about 300 K) and chemical reaction (begins at about 750 K). Defect sites in CNTs could adsorb hydrogen molecules accompanying a considerable increase in both the adsorption binding energy of the order of 50% and desorption temperature, which will definitely affect the molecular hydrogen storage capacity in carbon nanotubes in comparison to ideal hexagonal structures of CNTs.[41,42] According to above reports, binding between the carbon atoms and H_2 molecules adsorped in the MWCNTs (Figure 7) is taken into account as a type of physical adsorption and not chemisorption of C−H bonds. Singh et al.[52] investigated storage capacity based on of C−H_2 interaction potential and C−H_2 binding energy. They considered two different C−H_2 potentials for H_2 physisorbed on graphite, as Wang potential (12−6 Lennard-Jones potential) and Patchkovskii potential. In spite of their similarities, the Patchkovskii potential gives a stronger C−H_2 binding and results in higher absorption compared to the more conservative results obtained with the potential of Wang et al. Accordingly, they call them strong and weak interactions, and the storage capacities obtained by using these two potentials offer the upper and the lower bonds for the expected realistic experimental range. Their results showed that the storage capacities of carbon foams with the quantum corrected potentials were about 2.45 and 3.18 wt % for weak and strong potentials at 298 K. Studies also indicated that H atoms or protons have smaller diameter and lower resistance effects that can easily penetrate into tube walls while the diffusion of hydrogen molecules via sp^2 structure are very difficult unless some defects exist in the graphitized layers.[25,50]

Therefore, we believe that hydrogen molecules are adsorbed on the defect sites and transported to the spaces between adjacent carbon layers of MWCNTs via diffusion of defect sites as well as the opened tips of pure MWCNTs. Finally, they are stored on the sp^2 structures (first desorption temperature) and defect sites (second desorption temperature) by means of the physical adsorption. Defect sites enhance binding energy between C atoms and H_2 molecules accordingly.[41,42] Sha et al.[32] explained that H_2 molecular diffusion through the slit pours into the bulk BC_3 lattice would be facile under near-ambient conditions. Therefore, several reports are available to confirm our proposed mechanism as H_2 molecular storage for pure MWCNTs.[25,32,50]

On the other hand, the desorption temperature and hydrogen storage capacity in both regions notably increase in the decorated MWCNTs by Ca, Co, Fe, and Ni atoms in comparison to pure MWCNTs. Liu et al.[35] reported a high uptake H_2 capacity of 13.45 wt % for Li-dispersed carbon nanotubes system using density functional theory (DFT) calculations. Adsorption energy (E_{ad}) values of H_2/C_{64}, $H_2/Li/C_{64}$, and $H_2/Li_8/C_{64}$ systems were −0.10, −0.24, and −0.30 eV/H_2, respectively. Thus, the binding strength and uptake capacity of the carbon nanotubes can be enhanced by introducing more dopants due to electron transfer from Li atoms to carbon atoms. This finding was also reported for Ca[34,36] and transition metals[37] by the other researchers. Many studies have also revealed that hydrogen storage by hydrogen spillover on the added metal nanoparticles to CNTs is a promising approach to enhance the adsorption and storage of hydrogen in CNTs.[13−16] Kim et al. reported that Ni catalysts have been known to effectively dissociate hydrogen molecules in the gas phase, providing atomic hydrogen possible to form chemical bonding with the surfaces of MWCNTs.[31] Furthermore, between strong chemisorptions and weak physisorption states, there exists a Kubas type of interaction, a "nonclassical" form of binding of H_2 to metal with a binding energy in the range of 0.2−0.7 eV/H_2, which is ideal for the reversible storage at ambient conditions.[34,37,43] A single metal atom can bind multiple H_2 molecules via the Kubas interaction, leading to high gravimetric and volumetric density. Singh et al.[34] reported the high hydrogen storage capacity of metallacarboranes, which the light transition metal (TM) atoms can bind up to five H_2-molecules via the Kubas interaction. Similar results were obtained by studies of hydrogen adsorption capacity of SWCNTs, C_{60}, graphene, and other carbon-based structures decorated by light TM such as Ni, Sc, Fe, Co, and V.[53−56] Those suggest that the modified carbon materials can bind as many as five H_2 molecules per TM atom. Kim et al.[43] illustrated that Ca atoms decorated to graphene-based three-dimensional structures adsorbed H_2 molecules via the Kubas interaction. The hydrogen storage gravimetric capacity reaches about 5−6 wt %.

To our knowledge, there are likely a couple of mechanisms for Co, Fe, Ni, and Ca metals that used as dopants to purified MWCNTs: one involves adsorption of the several hydrogen molecules via Kubas interaction, while the second explains by dissociation of H_2 molecules on the metal particles and atomic H spills over to the spaces between adjacent carbon layers of MWCNTs. The binding energy between atomic H and carbon

atoms improved due to electron transfer from metal atoms to carbon atoms.[34−37] Wang et al.[36] have also reported that $C_{60}Ca_{32}$ bind up to 6.2 wt % hydrogen with the first 3 wt % bound atomically with a reduced binding energy of 0.45 eV/H and the remaining 3.2 wt % quasi-molecularly (Kubas interaction) with a binding energy of 0.11 eV/H_2.

Durgun et al.[57] studied that heavier metals such as Pd and Pt can also form complexes with C_2H_4 while bind fewer hydrogen molecules (two molecules) with significantly stronger binding energy than Ti. This is not exactly the case here because the hydrogen storage capacity in the Pd-MWCNTs is about 7 wt % reported but hydrogen storage capacity in the Pd-MWCNTs is less than 2 wt % via Kubas interaction, which denotes several times smaller than our experimental values. On the other hand, Yildirim et al.[53,58] have proposed that both filled and empty d orbitals are necessary for the metal−H_2 complex formation on decorated CNTs. Consequently, heavy transition metals such as Pt and Pd are not considered as good candidates for the molecular absorption via the Kubas interaction. In addition, experimental evidence suggests that the enhancement of hydrogen storage capacity in Pd-doped carbon nanostructures involves the dissociation of H_2 molecule on the decoration, followed by the atomic hydrogen spillover and adsorption processes on the carbon surface.[53,59−62] Nevertheless, H_2 adsorption on Pd-functionalized carbon nanomaterials still suffers lack of a consistent theory.[59,60] Forthermore, Lipson et al.[60] discussed electrochemical loading of SWCNTs encapsulated by thin Pd coating leading to an H_2 storage capacity of 8−12 wt % in ambient conditions. They have found that H loading into the Pd at temperatures above 290 K does not appear in the activation-dependent curve since the phase in PdH_x cannot thermally decompose below temperature of 400 K. Therefore, the enhancement of the hydrogen storage capacity in the Pd-CNTs will not be due to the formation of PdH_x[60] and C−H compositions.[50] They suggested that the enhancement of storage capacity arises from the fact that atomic hydrogen moves through the PdH_x into the SWCNT openings which permeate the interior of the nanotube, resulting in the formation of a Pd−C−H_x type charge-transfer complex.

Therefore, on the basis of several evidences above, we believe that H_2 is dissociated by the Pd particles on the defect sites (see results of TEM and XPS analyses) and leading to the subsequent hydrogen storage in the Pd-MWCNTs systems. The atomic hydrogen then spills over to the receptor (MWCNTs) via surface diffusion of sp^2 structures and defect sites.[13,14] The dominant mechanisms could be either the adsorption of the H atoms on the defect sites (CH_x) or the formation of Pd−C−H_x complex. These interactions must be accompanied by an electron transfer from metal atoms to carbon atoms.[37,61] However, those are loose bonds which can be easily decomposed at lower temperatures compared to much stronger C−H chemical bonds. To understand why Pd is more effective in H_2 dissociation as compared to other metals, we have studied and compared physical and chemical properties for the investigated metal-doped MWCNTs systems. On the basis of the comparison, it was found that sticking probability, diffusion coefficient, and Binding energy between atomic H and Pd atoms are the largest for Pd metal and smallest for Ni metal.[63−67]

4. CONCLUSIONS

We have explored that there are a couple of regions for hydrogen adsorption on purified MWCNTs: one is corresponding to the interaction of H_2 molecules with sp^2 configuration of carbon nanotubes, and the other is related to the interaction of H_2 molecules with defect sites. The results showed that hydrogen molecules are adsorbed on the defect sites and transport into the spaces between adjacent carbon layers of the purified MWCNTs through hydrogen diffusion via both defect sites and the opened tips of purified MWCNTs. Binding energy and hydrogen storage capacity in these sites are increased in the decorated MWCNTs by Ca, Co, Fe, Ni, and Pd particles compared to the purified MWCNTs mainly due to the electron transfer from metal atoms to carbon atoms. It was also found that Pd particles in the defect sites dissociate H_2 molecules on their surface, resulting in the highest level of hydrogen storage in the spaces between adjacent carbon layers. The dominant mechanism in the adsorption of atomic hydrogen in the Pd-decorated MWCNTs could be either adsorption of the H atoms on the defect sites forming CH_x species or Pd−C−H_x complex.

AUTHOR INFORMATION

Corresponding Author

*Tel +98-21-6600-5410, Fax +98-21-6601-2983, e-mail moshfegh@sharif.edu.

ACKNOWLEDGMENT

The authors thank the Research and Technology Council of Sharif University of Technology and Materials Research School for their cooperation and support.

REFERENCES

(1) Mpourmpakis, G.; Tylianakis, E.; Froudakis, G. E. *Nano Lett.* **2007**, *7*, 1893–7.
(2) Bilic, A.; Gale, J. D. *J. Phys. Chem. C* **2008**, *112*, 12568–75.
(3) Fang, B.; Zhou, H.; Honma, I. *J. Phys. Chem. B* **2006**, *110*, 4875–80.
(4) Schlapbach, L.; Züttel, A. *Nature* **2001**, *414*, 353–8.
(5) Vajo, J.; Pinkerton, F.; Stetson, N. *Nanotechnology* **2009**, *20*, 200201–2.
(6) Lee, H.; Ihm, J.; Cohen, M. L.; Louie, S. G. *Nano Lett.* **2010**, *10*, 793–8.
(7) Burress, J.; Kraus, M.; Beckner, M.; Cepel, R.; Suppes, G.; Wexler, C.; Pfeifer, P. *Nanotechnology* **2009**, *20*, 204026–35.
(8) Dillon, A. C.; Jones, K. M.; Bekkedahl, T. A.; Kiang, C. H.; Bethune, D. S.; Heben, M. J. *Nature* **1997**, *386*, 377–9.
(9) Kai, S.; Huafang, X.; Yingbin, J.; Tanja, P. *Carbon* **2004**, *42*, 2315–22.
(10) Thomas, K. M. *Catal. Today* **2007**, *120*, 389–98.
(11) Patchovskii, S.; Tse, J. S.; Yurchenko, S. N.; Zhechkov, L.; Heine, T.; Seifert, G. *Proc. Natl. Acad. Sci. U.S.A.* **2005**, *102*, 10439–44.
(12) Ferro, Y.; Marinelli, F.; Allouche, A.; Brosset, C. *J. Chem. Phys.* **2003**, *118*, 5650–7.
(13) Wang, L.; Yang, R. T. *J. Phys. Chem. C* **2008**, *112*, 12486–94.
(14) Lachawiec, A. J.; Qi, J. G.; Yang, R. T. *Langmuir* **2005**, *21*, 11418–24.
(15) Reyhani, A.; Mortazavi, S. Z.; Moshfegh, A. Z.; Nozad Golikand, A.; Amiri, M. *J. Power Sources* **2009**, *188*, 404–10.
(16) Yoo, E.; Komatsu, T.; Yagai, N.; Arai, K.; Yamazaki, T.; Matsuishi, K.; Matsumoto, T.; Nakamura, J. *J. Phys. Chem. B* **2004**, *108*, 18903–7.
(17) Suttisawat, Y.; Rangsunvigit, P.; Kitiyanan, B.; Williams, M.; Ndungu, P.; Lototskyy, M. V.; Nechaev, A.; Linkov, V.; Kulprathipanja, S. *Int. J. Hydrogen Energy* **2009**, *34*, 6669–75.
(18) Zacharia, R.; Kim, K. Y.; Fazle Kibria, A. K. M.; Nahm, K. S. *Chem. Phys. Lett.* **2005**, *412*, 369–75.

(19) Gao, L.; Yoo, E.; Nakamura, J.; Zhang, W.; Chua, H. T. *Carbon* **2010**, *48*, 3250–55.
(20) Hwang, S. W.; Rather, S. U.; Naik, M. U. D.; Soo, C. S.; Nahm, K. S. *J. Alloys Compd.* **2009**, *480*, L20–L24.
(21) Ferre-Vilaplana, A. *J. Phys. Chem. C* **2008**, *112*, 3998–4004.
(22) Klontzas, E.; Mavrandonakis, A.; Tylianakis, E.; Froudakis, G. E. *Nano Lett.* **2008**, *8*, 1572–6.
(23) Rather, S. U.; Naik, M. U. D.; Hwang, S. W.; Kim, A. R.; Nahm, K. S. *J. Alloys Compd.* **2009**, L17–L21.
(24) Campesia, R.; Cuevasa, F.; Gadioub, R.; Leroya, E.; Hirscherc, M.; Vix-Guterl, C.; Latrochea, M. *Carbon* **2008**, *46*, 206–14.
(25) Mu, S. C.; Tang, H. L.; Qian, S. H.; Pan, M.; Yuan, R. Z. *Carbon* **2006**, *44*, 762–7.
(26) Chang, J. K.; Chen, C. Y.; Tsai, W. T. *Nanotechnology* **2009**, *20*, 495603–10.
(27) Park, S. J.; Lee, S. Y. *Int. J. Hydrogen Energy* **2010**, *35*, 13048–54.
(28) Leela Mohana Reddy, A.; Ramaprabhu, S. *Int. J. Hydrogen Energy* **2007**, *32*, 3998–4004.
(29) Rather, S. U.; Mehraj-ud-din, N.; Zacharia, R.; Hwang, S. W.; Kim, A. R.; Nahm, K. S. *Int. J. Hydrogen Energy* **2009**, *34*, 961–966.
(30) Li, Y.; Yang, R. T. *Ind. Eng. Chem. Res.* **2007**, *46*, 8277–81.
(31) Kim, H. S.; Lee, H.; Han, K. S.; Kim, J. H.; Song, M. S.; Park, M. S.; Lee, J. Y.; Kang, J. K. *J. Phys. Chem. B* **2005**, *109*, 8983–6.
(32) Sha, X.; Cooper, A. C.; Bailey, W. H.; Cheng, H. *J. Phys. Chem. C* **2010**, *114*, 3260–4.
(33) Wang, L.; Lee, K.; Sun, Y. Y.; Lucking, M.; Chen, Z.; Zhao, J. J.; Zhang, S. B. *ACS Nano* **2009**, *3*, 2995–3000.
(34) Singh, A. K.; Sadrzadeh, A.; Yakobson, B. I. *J. Am. Chem. Soc.* **2010**, *132*, 14126–9.
(35) Liu, W.; Zhao, Y. H.; Li, Y.; Jiang, Q.; Lavernia, E. J. *J. Phys. Chem. C* **2009**, *113*, 2028–33.
(36) Wang, Q.; Sun, Q.; Jena, P.; Kawazoe, Y. *J. Chem. Theory Comput.* **2009**, *5*, 374–9.
(37) Bhattacharya, A.; Bhattacharya, S.; Majumder, C.; Das, G. P. *J. Phys. Chem. C* **2010**, *114*, 10297–301.
(38) Reyhani, A.; Mortazavi, S. Z.; Moshfegh, A. Z.; Nozad Golikand, A. *Int. J. Hydrogen Energy* **2010**, *35*, 231–7.
(39) Reyhani, A.; Nozad Golikand, A.; Mortazavi, S. Z.; Irannejad, L.; Moshfegh, A. Z. *Electrochim. Acta* **2010**, *55*, 4700–5.
(40) Jorio, A.; Pimenta, M. A.; Souza Filho, A. G.; Saito, R.; Dresselhaus, G.; Dresselhaus, S. *New J. Phys.* **2003**, *5*, 139.1–139.17.
(41) Wu, H.; Wexler, D.; Ranjbartoreh, A. R.; Liu, H.; Wang, G. *Int. J. Hydrogen Energy* **2010**, *35*, 6345–9.
(42) Gayathri, V.; Geetha, R. *Adsorption* **2007**, *13*, 53–9.
(43) Kim, G.; Jhi, S. H. *J. Phys. Chem. C* **2009**, *113*, 20499–503.
(44) Itoh, T.; Urita, K.; Bekyarova, E.; Arai, M.; Yudasaka, M.; Iijima, S.; Ohba, T.; Kaneko, K.; Kanoh, H. *J. Colloid Interface Sci.* **2008**, *322*, 209–14.
(45) Kim, D. Y.; Yang, C. M.; Noguchi, H.; Yamamoto, M.; Ohba, T.; Kanoh, H.; Kaneko, K. *Carbon* **2008**, *46*, 611–7.
(46) Okpalugo, T. I. T.; Papakonstantinou, P.; Murphy, H.; McLaughlin, J.; Brown, N. M. D. *Carbon* **2005**, *43*, 153–61.
(47) Zuttel, A.; Sudan, P.; Mauron, Ph.; Kiyobayashi, T.; Emmenegger, Ch.; Schlapbach, L. *Int. J. Hydrogen Energy* **2002**, *27*, 203–12.
(48) Anson, A.; Benham, M.; Jagiello, J.; Callejas, M. A.; Benito, A. M.; Maser, W. K.; Uttel, A. Z.; Sudan, P.; Martınez, M. T. *Nanotechnology* **2004**, *15*, 1503–8.
(49) Alberty, R. A.; Silbey, R. J. *Physical Chemistry*; Wiley: New York, 1997.
(50) Nikitin, A.; Li, X.; Zhang, Z.; Ogasawara, H.; Dai, H.; Nilsson, A. *Nano Lett.* **2008**, *8*, 162–7.
(51) Lee, S. M.; An, K. H.; Lee, Y. H.; Seifert, G.; Frauenheim, T. *J. Am. Chem. Soc.* **2001**, *123*, 5059–63.
(52) Singh, A. K.; Lu, J.; Aga, R. S.; Yakobson, B. I. *J. Phys. Chem. C* **2011**, *115*, 2476–82.
(53) Yildirim, T.; Iniguez, J.; Ciraci, S. *Phys. Rev. B* **2005**, *72*, 153403.
(54) Zhao, Y. F.; Kim, Y. H.; Dillon, A. C.; Heben, M. J.; Zhang, S. B. *Phys. Rev. Lett.* **2005**, *94*, 155504.
(55) Lee, J. W.; Kim, H. S.; Lee, J. Y.; Kang, J. K. *Appl. Phys. Lett.* **2006**, *88*, 143126.
(56) Durgun, E.; Ciraci, S.; Yildirim, T. *Phys. Rev. B* **2008**, *77*, 85405.
(57) Durgun, E.; Ciraci, S.; Zhou, W.; Yildirim, T. *Phys. Rev. Lett.* **2006**, *97*, 226102–5.
(58) Yildirim, T.; Ciraci, S. *Phys. Rev. Lett.* **2005**, *94*, 175501.
(59) Lopez-Corral, I.; German, E.; Volpe, M. A.; Brizuela, G. P.; Juan, A. *Int. J. Hydrogen Energy* **2010**, *35*, 2377–84.
(60) Lipson, G.; Lyakhov, B. F.; Saunin, E. I.; Tsivadze, A. Y. *Phys. Rev. B* **2008**, *77*, 081405–9.
(61) Yang, R. T.; Wang, Y. *J. Am. Chem. Soc.* **2009**, *131*, 4224–6.
(62) Wang, Z.; Yang, R. T. *J. Phys. Chem. C* **2010**, *114*, 5956–63.
(63) Nieuwenhuys, B. E. *Surf. Sci.* **1983**, *126*, 307–36.
(64) Johansson, M.; Skúlason, E.; Nielsen, G.; Murphy, S.; Nielsen, R. M.; Chorkendorff, I. *Surf. Sci.* **2010**, *604*, 718–29.
(65) Johansson, M.; Lytken, O.; Chorkendorff, I. *Surf. Sci.* **2008**, *602*, 1863–70.
(66) Osing, J.; Murphy, S.; Shvets, I. V. *Surf. Sci.* **2000**, *454–456*, 280–3.
(67) Ingrin, J.; Blanchard, M. *Rev. Mineral. Geochem.* **2006**, *62*, 291–320.